Mon. Not. R. astr. Soc. (1975) **171**, 475–505.

THE 5C 5 SURVEY OF RADIO SOURCES

T. J. Pearson

Mullard Radio Astronomy Observatory, Cavendish Laboratory, Cambridge

(Communicated by G. G. Pooley)

(Received 1975 January 27; in original form 1974 December 20)

SUMMARY

The 5C 5 survey, made with the Cambridge One-Mile telescope, covers an area about 4° in diameter at 408 MHz centred at $\alpha = 09^h\,40^m$, $\delta = 47°\,00'$ to a limiting flux density of $8{\cdot}7 \times 10^{-29}$ W m^{-2} Hz^{-1} at the centre, and a concentric area of diameter about 1° at 1407 MHz to a limiting flux density of $1{\cdot}8 \times 10^{-29}$ W m^{-2} Hz^{-1}. The positions and flux densities of 230 sources observed at 408 MHz, and of 52 observed at 1407 MHz, are listed in Table I, with suggested optical identifications for some of the sources. The flux density and spectral index distributions are similar to those of the earlier 5C surveys and there is no evidence for significant anisotropy in either distribution. New observations of some 5C 1 sources included in the 5C 5 survey show that the flux densities measured in 5C 1 were in error.

1. INTRODUCTION

This fifth Cambridge deep survey of weak radio sources was undertaken in order to improve the statistics of the flux density distribution of sources at the lowest detectable levels, and to determine whether or not the 5C 2 survey (Pooley & Kenderdine 1968), the results of which have been extensively used in observational cosmology, provides a fair sample of these faint sources ($S_{408} \gtrsim 10^{-28}$ W m^{-2} Hz^{-1}). Of the four previous 5C surveys, 5C 3 (Pooley 1969) and 5C 4 (Willson 1970) were of atypical areas of sky centred on M31 and on the Coma cluster of galaxies respectively; and the 5C 1 and 5C 2 surveys, although of areas of sky exceptional only for the absence of bright sources, were not strictly comparable with each other, owing to instrumental differences. 5C 1 (Kenderdine, Ryle & Pooley 1966) was the first survey to be made with a new instrument, and suffered from severe terrestrial radio interference and from an offset primary reception pattern; it was also less sensitive than the 5C 2 survey. Pooley & Ryle (1968) excluded 5C 1 from their compilation of 408 MHz source counts for these reasons. A comparison of the results of 5C 1 and 5C 2 (Maslowski 1972a, 1974) suggests that there is anisotropy in the source distribution, but this effect may be due in part to the instrumental differences, and has been questioned on these grounds (Condon & Jauncey 1973).

The 5C 5 survey was centred 3° south of the nominal centre of the 5C 1 survey, with about 30 per cent of its area in common with 5C 1, enabling the 5C 1 results to be checked. The new survey is more nearly comparable, in its instrumental properties, with 5C 2, 5C 3 and 5C 4 than is 5C 1, and its results are to be preferred to those of 5C 1 for any statistical investigations. There is no evidence from a

comparison of the flux density distribution or spectral index distribution of 5C 5 with those of 5C 2 for any significant difference in the distribution of sources between these two areas; a comparison with 5C 1, however, has revealed errors in the 5C 1 408 MHz flux densities.

The methods of observation and data reduction are described in Sections 2 and 3, and a list of the radio sources observed is given in Table I. The measurements of flux density and position are compared with those of 5C 1 in Section 4. The statistical results of the survey, and their comparison with other observations, can be found in Section 7 (source counts) and Section 8 (spectra).

2. OBSERVATIONS

As in the previous 5C surveys, the Cambridge One-Mile telescope was used to observe simultaneously at 408 MHz a field approximately 4° in diameter, and at 1407 MHz a concentric field approximately 1° in diameter. The field centre was $\alpha = 09^h\,40^m\,00^s$, $\delta = 47°\,00'$ (1950·0). This region is free from intense sources (there are no 4C sources in the field, with the exception of 4C 48.26 on the extreme western margin).

The technical details of the observations were similar to those of the previous 5C surveys (described by Kenderdine, Ryle & Pooley 1966; Pooley & Kenderdine 1968) and will be only briefly summarized here. A circular aperture was synthesized from 12-hr runs at each of 127 different aerial separations, ranging from a minimum of 35·2 m to a maximum of 1513·8 m (=2060 λ at 408 MHz, 7100 λ at 1407 MHz) in steps of 11·7 m. The aperture grading was the usual gaussian function falling to 0·3 of its maximum at the largest aerial separation, so that the synthesized beam (which is elliptically symmetrical, with its major axis in the declination direction) had a half-power width $80'' \times 109''$ (408 MHz) or $23'' \times 31''$ (1407 MHz). With this grading, none of the sidelobes exceeds 6 per cent of the maximum, with the exception of a series of 'grating rings' whose radii are multiples of $1/D$, where D is the spacing increment in wavelengths. As in the previous surveys, the first grating ring of a source at one edge of the map appears near the opposite edge. At 408 MHz, some of the observations had to be omitted from the analysis because of terrestrial radio interference; this had little effect on the shape of the synthesized beam, but necessitated a correction of about 3·5 per cent to the observed flux densities.

The observations were made in 1973 March–May using new feed assemblies which accepted linearly polarized radiation with the **E**-vector in p.a. 0° at both frequencies. The new first-stage amplifiers at each aerial were, at 408 MHz, a bipolar transistor r.f. amplifier giving a system noise temperature of about 160 K; and, at 1407 MHz, a Ferranti non-degenerate parametric amplifier pumped at 17 GHz giving a system noise temperature of about 115 K. The bandwidths were 4 MHz at 408 MHz and 10 MHz at 1407 MHz. The sensitivity at 408 MHz was similar to that of the earlier 5C surveys: the rms noise level on the map (before correction for the primary aerial envelope response) was about $1{\cdot}7 \times 10^{-29}$ W m^{-2} Hz^{-1} per beam area (*cf.* $1{\cdot}6 \times 10^{-29}$ W m^{-2} Hz^{-1} for 5C 2). Of this the system noise temperature contributes $0{\cdot}5 \times 10^{-29}$ W m^{-2} Hz^{-1}, and sources below the limiting flux density of the survey $0{\cdot}2 \times 10^{-29}$ W m^{-2} Hz^{-1}. The largest contribution to the noise is made by the sidelobes of the stronger sources and grating rings of sources outside the mapped area. Unfortunately it was not possible to improve the noise

level by removing sources and their associated sidelobes owing to the large amount of computing time that would have been required, and because the accuracy with which sidelobes can be eliminated is limited by instrumental instabilities to about 0·5 per cent of the flux density of the strongest sources, that is, about $1{\cdot}5 \times 10^{-29}$ W m^{-2} Hz^{-1}. At 1407 MHz, confusion by sidelobes is less important, the system noise contributing $0{\cdot}22 \times 10^{-29}$ W m^{-2} Hz^{-1} to the total rms noise level of $0{\cdot}35 \times 10^{-29}$ W m^{-2} Hz^{-1}. This figure is an improvement on the earlier surveys (e.g. 5C 2: $1{\cdot}5 \times 10^{-29}$ W m^{-2} Hz^{-1}) owing to the improved first-stage amplifier and the larger bandwidth; consequently more sources have been detected at 1407 MHz than were before. In order to reduce confusion by sidelobes at this frequency, most of the analysis was done on a map with the strong source 5C 5.175 removed by the procedure of Neville, Windram & Kenderdine (1969). The maps were made by the same Fourier Transform techniques as the earlier 5C maps; they represent the sky brightness attenuated towards the edge of the map by the envelope response of the individual dishes, and by other effects mentioned in Section 3.2.

3. SOURCE LIST

The coordinates (reduced to 1950·0) and flux densities of all the sources found in the survey with apparent intensities (before correction for the envelope response) $S'_{408} > 8{\cdot}7 \times 10^{-29}$ W m^{-2} Hz^{-1} or $S'_{1407} > 1{\cdot}8 \times 10^{-29}$ W m^{-2} Hz^{-1} are listed in Table I. The positions and flux densities of unresolved sources were determined with the beamshape-fitting program used in the earlier surveys; sources which could not be fitted closely to the ideal beamshape, or which appeared resolved on contour maps, were treated separately. A number of spurious sources, arising from the intersection of grating rings or sidelobes of bright sources, were eliminated by hand.

3.1 *Positions*

The positions of the sources found at 408 MHz were adjusted by the mean difference between the 408 and 1407 MHz positions of 18 unresolved sources observed at both frequencies ($+0^{s}{\cdot}32 \pm 0^{s}{\cdot}05$, $+0''{\cdot}8 \pm 1''{\cdot}1$); this difference is due mostly to ionospheric refraction, which has only a small effect ($\sim 0''{\cdot}1$ arc) at the higher frequency. For sources observed at both frequencies the positions given are those derived from the 1407 MHz map. The coordinates of resolved sources were measured from contour maps; they refer to the peaks of radio brightness. Such sources are marked ' e ' (' extended ') in Table I.

The positional uncertainties attributable to noise and confusion were estimated as a function of uncorrected flux density by a Monte Carlo method (Kenderdine *et al.* 1966). The rms uncertainty in right ascension for each source is given in Table I (column 4) in arcsec; the uncertainties in declination are greater by a factor cosec (δ) = 1·37. These estimated errors do not include systematic effects, among which are the following:

(i) The effect of an asymmetry in the beamshape (ignored in the source-finding program) due to phase errors or to the holes in the aperture left after the removal of interference. Any such fitting error is small at 1407 MHz ($< 0''{\cdot}1$ arc) and at 408 MHz it is mostly removed by the ionospheric refraction correction mentioned above. Because it is impossible to adjust the path compensators correctly for all parts of the map, the finite bandwidth introduces an attenuation which varies with

TABLE I

5C 5	R.A. (1950) h m s	Dec. (1950) ° ′ ″	R.A. error ″	S_{408} (10^{-29} W m^{-2} Hz^{-1})	S_{1407} (10^{-29} W m^{-2} Hz^{-1})	Spectral index	Notes
1	09 28 13.3	48 4 36	e	2584	*		4C48.26 Two components: Np:Sf = 1.2:1
2	28 15.5	48 2 57	e				
3	29 12.3	47 50 58	8	86	27		
4	29 53.6	46 28 44	7	61	14		
5	29 56.0	47 0 20	2	193	27		
6	09 30 3.0	47 52 26	1	681	123		5C1.5
7	30 11.4	48 1 11	2	253	51		5C1.6
8	30 12.3	47 30 7	9	42	11		
9	30 18.5	49 3 13	1	710	*		5C1.7 Part of KPD3
10	30 26.3	47 54 18	8	51	14		Confused by sidelobe of 6
11	09 30 35.8	45 33 10	1	637	187		
12	30 43.1	47 23 21	8	39	9		
13	30 54.8	48 55 51	4	383	*		5C1.11
14	30 55.0	49 21 34	1	470	*		5C1.12 KPD4; S(5000)=440 (5-km)
15	30 57.5	47 8 23	9	29	8		
16	09 30 58.6	46 5 4	3	149	23		
17	31 35.0	46 16 37	8	33	8		
18	31 35.2	48 25 20	7	81	21		
19	32 4.3	46 36 41	1	557	45		
20	32 30.2	48 12 53	2	142	20		5C1.22
21	09 32 53.9	46 32 5	5	33	5		
22	33 4.3	48 57 18	5	184	*		5C1.28
23	33 6.6	45 39 1	2	216	28		
24	33 13.4	45 11 11	1	522	127		
25	33 16.2	46 42 5	4	45	5		

1975MNRAS.171..475P

26	09	33	18.2	48	41	28	6	83	20
27		33	18.5	44	46	28	7	222	*
28		33	21.4	44	57	30	5	177	*
29		33	24.3	47	2	6	8	20	4
30		33	26.1	47	16	18	4	43	5
31	09	33	36.8	47	7	9	3	46	5
32		33	51.1	46	57	46	3	50	4
33		33	56.9	47	12	28	e	58	8
34		34	0.5	46	30	29	2	81	6
35		34	6.1	46	22	32	2	82	6
36	09	34	13.2	47	36	27	4	35	4
37		34	17.4	47	15	54	1	283	15
38		34	31.1	47	55	29	e	213	25
39		34	38.2	45	25	35	4	77	13
40		34	40.2	48	10	56	8	26	6
41	09	34	49.2	46	5	26	7	24	5
42		35	0.9	47	25	35	1	226	11
43		35	0.9	47	4	7	7	17	3
44		35	9.9	45	59	15	7	26	5
45		35	10.5	49	30	16	e	768	*
46	09	35	21.9	45	33	53	1	549	52
47		35	27.5	45	4	11	3	149	31
48		35	32.2	47	11	37	2	54	4
49		35	37.0	47	17	48	e	35	6
50		35	55.2	48	3	53	7	22	4

5C1.31

Confused by sidelobe of 37; slightly extended NE-SW

ARG 1 Extended 1'.5 towards E

ARG 3

5C1.38 ARG 4 Component 2' W with 0.3 of flux density; KPD6

Slightly extended

Slightly extended

TABLE I—*continued*

5C 5	R.A. (1950) h m s	Dec. (1950) ° ′ ″	R.A. error ″	S_{408} (10^{-29} W m^{-2} Hz^{-1})	S_{1407}	Spectral index	Notes
51	09 36 0.8	46 2 8	2	60 5			
52	36 3.5	47 54 51	3	42 4			ARG 5
53	36 5.9	46 47 42	2	63 4			
54	36 9.5	48 8 18	5	35 5			ARG 6
55	36 12.0	46 11 14	7	19 3			
56	09 36 15.7	44 55 32	7	91 25			
57	36 15.8	46 42 52	1	152 6			
58	36 17.3	48 38 44	6	52 9			5C1.44 ARG 7
59	36 18.8	45 3 32	2	199 36			
60	36 18.9	47 0 39	1	180 7			
61	09 36 33.8	47 56 3	1	100 6			ARG 8
62	36 41.3	48 4 14	2	92 6			ARG 9
63	36 45.2	47 51 37	1	154 8			5C1.48 ARG 10
64	36 47.0	47 18 29	8	13 3			
65	36 47.2	46 30 42	4	28 3			
66	09 36 48.7	48 40 25	4	71 11			5C1.50 ARG 11
67	36 55.7	47 9 48	9	11 2			
68	36 59.8	46 7 28	8	16 3			
69	37 0.3	45 57 24	5	28 4			
70	37 4.9	47 55 4	6	21 6			Confused, perhaps extended
71	09 37 8.6	46 52 25	4	21 3			
72	37 20.0	47 15 23	8	11 3			Slightly extended ?
73a	37 20.44	47 4 25.3	e	248 40	94.4 18	0.78	Confused at 408 by sidelobe of 80;
b	37 23.20	47 4 55.0	e				two components at 1407: a:b = 3:4
74	37 20.8	46 36 49	9	11 3			
75	37 22.6	48 26 11	1	144 12			5C1.54 ARG 13

76	09	37 26.9	46 14 1	3	44	3					
77		37 29.8	46 2 26	3	42	4					
78		37 33.0	47 40 29	4	29	3					
79		37 35.24	46 57 52.2	2.0	17	2	5.6	1.1	0.89	Confused at 408	
80		37 37.52	47 3 21.3	0.2	136	5	139.8	11.0	-0.02	Slightly confused by sidelobe of 73 at 408	
81	09	37 40.3	46 15 45	6	18	3					
82		37 41.4	47 50 36	4	27	3					
83		37 42.4	47 43 10	2	45	3					
84		37 42.6	45 17 32	6	43	8					
85		37 44.8	46 7 14	8	15	3					
86	09	37 54.6	47 19 1	8	12	2				Confused by grating ring of 3C219	
87		37 55.1	47 56 25	1	472	22				5C1.56 ARG 16	
88		37 57.3	45 48 25	5	32	4					
89		38 0.34	47 7 38.9	1.3			6.8	0.9			
90		38 10.5	48 34 16	1	345	30				5C1.58 ARG 18 KPD8 S(5000)=80	
91	09	38 15.32	47 3 38.5	0.9	28	2	8.2	0.8	1.00		
92		38 16.5	46 7 18	1	120	6					
93		38 16.9	49 12 36	9	73	24				5C1.59	
94		38 17.4	45 1 28	2	180	29				Confused by grating ring of 3C219	
95		38 19.1	49 7 13	5	110	26				5C1.60 ARG 20	
96	09	38 19.42	47 19 49.5	1.1	23	2	10.4	1.3	0.66		
97		38 22.6	46 50 23	8	11	3				Confused by grating ring of 3C219	
98		38 23.24	47 6 25.9	2.3			3.1	0.6			
99		38 25.3	47 46 7	8	13	3					
100		38 31.0	46 32 59	5	18	2					

TABLE I—*continued*

5C 5	R.A. (1950) h m s	Dec. (1950) ° ′ ″	R.A. error ″	S_{408} (10^{-29} W m^{-2} Hz^{-1})		S_{1407}		Spectral index	Notes
101	09 38 33.87	47 3 25.3	1.7			3.8	0.6		
102	38 37.9	46 9 6	8	14	3				Confused by sidelobe of 123
103	38 46.4	46 42 29	7	13	2				
104	38 48.2	48 18 28	1	237	15				5C1.63 ARG 23
105	38 50.5	47 53 29	9	13	3				
106	09 38 50.7	49 3 4	1	323	56				5C1.64 ARG 24
107	38 51.40	47 10 48.2	0.5	53	3	13.8	0.8	1.09	
108	38 52.9	48 14 35	7	21	4				Confused by sidelobes of 104 and 116
109	38 53.3	46 19 25	6	16	3				
110	38 54.8	45 33 25	4	45	6				
111	09 38 55.25	46 41 3.6	2.2			3.8	0.8		
112	39 4.19	46 41 51.2	0.6			13.2	1.0		
113	39 6.0	46 5 44	8	14	3				Confused by sidelobe of 123
114	39 8.97	47 3 51.6	0.2	80	3	25.4	1.0	0.92	
115	39 9.29	47 16 30.5	0.8	31	2	9.0	0.7	1.01	
116	09 39 12.2	48 17 26	1	128	9				5C1.66 ARG 26
117	39 12.61	46 36 35.5	2.1	15	2	4.8	0.9	0.91	
118	39 17.65	47 8 53.9	2.1			2.4	0.4		
119	39 18.7	45 6 60	4	81	13				Slightly extended
120	39 19.90	46 53 14.0	e	21	2	8.1	1.2	0.78	Extended towards NW at 1407
121	09 39 22.52	46 39 0.5	1.8	14	2	4.7	0.7	0.91	Slightly extended at 1407 ?
122	39 23.0	45 26 44	8	26	6				
123	39 38.1	46 5 2	1	473	20				
124	39 42.12	47 12 33.8	2.3			2.2	0.4		
125	39 45.88	47 15 10.7	1.8	14	2	3.2	0.5	1.21	

126	09	39 48.1	47 55 13	1	106	5				ARG 27
127		39 51.7	46 27 2	9	11	2				
128		39 54.8	47 34 41	9	10	2				
129		39 57.37	47 18 9.4	2.1			2.9	0.5		
130		40 3.31	46 22 20.6	1.3	88	4	19.9	4.3	1.20	
131	09	40 20.10	46 47 17.9	0.2			64.6	2.4		S(5000)=78 (5-km)
132		40 20.43	46 57 41.9	1.9			2.3	0.4		
133		40 20.6	48 28 44	6	31	5				ARG 28
134		40 20.77	46 53 17.4	1.0	18	2	4.6	0.4	1.11	
135		40 22.6	46 1 4	6	19	3				
136	09	40 23.2	45 52 37	7	19	4				
137a		40 24.15	46 29 51.3	4.0	43	3	6.4	1.3		
b		40 24.25	46 30 39.0	1.5			8.5	1.3		
138		40 31.74	46 49 59.8	1.6			2.9	0.4		
139		40 36.23	46 26 9.1	2.2	10	2	8.0	1.8	0.20	
140		40 41.09	47 34 36.3	1.3	67	10	14.3	2.4	1.25	Small component 2' E at 408
141	09	40 44.6	46 37 4	9	10	2				
142		40 46.4	49 22 58	4	205	*				5C1.72 ARG 29 Slightly extended
143		40 51.19	46 57 55.0	0.7			6.0	0.4		
144		40 51.66	46 51 41.2	1.7			2.8	0.4		
145		40 54.0	45 44 43	5	34	4				
146	09	41 0.1	45 27 16	4	55	7				
147		41 0.18	47 20 1.3	1.8			4.1	0.6		
148		41 8.1	47 41 20	3	40	3				
149		41 8.09	47 9 53.1	1.6			3.2	0.4		
150		41 11.71	47 5 51.1	1.4			3.5	0.4		

TABLE I—*continued*

5C 5	R.A. (1950) h m s	Dec. (1950) ° ′ ″	R.A. error ″	S_{408} (10^{-29} W m^{-2} Hz^{-1})		S_{1407}		Spectral index	Notes
151	09 41 19.0	48 2 30	1	85	5				5C1.78 ARG 30
152	41 22.4	47 53 13	9	12	6				Confused by sidelobe of 161
153	41 23.70	46 52 38.6	0.2	53	3	66.2	2.5	-0.18	
154	41 25.2	48 43 9	6	46	8				5C1.80 ARG 31
155	41 25.6	45 59 56	3	39	4				
156	09 41 28.1	45 26 2	8	29	6				
157	41 33.88	47 13 54.0	0.5	32	2	12.5	0.8	0.75	
158	41 37.0	48 16 51	2	102	7				5C1.83 ARG 32
159	41 40.9	47 30 49	8	12	2				Slightly confused by 169
160	41 43.9	47 36 6	6	16	3				Confused by sidelobe of 169
161	09 41 47.2	47 58 32	1	256	12				5C1.84 ARG 33
162	41 52.44	46 47 36.1	1.6			4.5	0.6		
163	41 53.1	45 1 24	5	87	17				
164	41 54.45	46 38 19.2	0.7	48	3	15.2	1.5	0.93	
165	41 55.83	47 31 19.8	1.0			20.4	3.3	[see 169]	See map
166	09 42 0.7	46 55 1	8	11	4				Confused by sidelobe of 175
167	42 0.9	46 25 30	9	11	3				
168	42 1.05	46 34 31.9	0.7	72	3	21.4	3.0	0.98	Extended at 1407
169	42 3.70	47 32 21.1	e	197	33	48.9	11	0.85	ARG 35 Extended: see map; spectral index includes 165
170	42 15.7	46 11 16	3	38	3				
171	09 42 17.6	47 43 24	8	13	3				
172	42 19.0	47 41 18	7	15	3				Confused by 171
173	42 20.29	47 4 2.8	0.6	31	3	12.1	0.9	0.75	
174	42 23.97	46 52 45.5	1.8			4.4	0.7		Confused by sidelobe of 175
175	42 28.71	46 50 43.5	0.2	336	11	246.1	15.7	0.25	

176	09	42 32.06	47 19 54.6	1.3	23	3	10.2	1.5	0.64		
177		42 33.6	45 8 16	3	118	18					
178		42 36.4	46 58 35	4	21	2				Confused by sidelobe of 175	
179		42 40.1	45 48 26	2	74	6					
180		42 44.55	46 33 14.6	1.0	51	3	23.9	4.5	0.60		
181	09	42 47.6	48 39 51	4	74	10				ARG 37	
182		42 49.5	47 48 57	e	45	8				ARG 38 Extended: see map	
183		42 50.7	44 30 10	3	504	*					
184		42 52.8	49 8 5	5	127	32				5C1.86 ARG 39	
185		42 54.02	46 54 15.5	1.0	25	6	10.7	1.2	0.67	Confused at 408 by sidelobe of 175	
186	09	42 57.24	46 47 41.4	e	88	4	23.7	5.0	1.06	Extended at 1407; confused at 408	
187		42 57.47	47 20 41.0	2.3	28	3	7.7	1.8	1.04		
188		43 12.4	46 24 28	e	341	60				2nd component 1' NE of peak position	
189		43 13.6	46 52 40	3	28	3					
190		43 13.8	47 51 48	e	222	40				ARG 41 Extended: see contour map	
191	09	43 14.51	47 38 0.4	5	192	8	56	*		ARG 42 Confused by 192 at 408 and 80 at 1407	
192		43 14.1	47 41 11	1	103	5				Slightly confused by 191	
193		43 16.49	46 26 6.1	0.2			45	*			
194		43 19.1	46 11 4	2	75	5					
195		43 24.5	45 25 22	8	31	7					
196	09	43 28.8	47 13 4	7	14	3					
197		43 32.5	46 27 29	2	68	4					
198		43 37.6	45 40 37	e	89	21				Extended towards NW	
199		43 39.6	47 8 25	5	19	3					
200		43 42.7	46 50 47	4	22	3					

TABLE I—*continued*

5C 5	R.A. (1950) h m s	Dec. (1950) ° ′ ″	R.A. error ″	S_{408} (10^{-29} W m^{-2} Hz^{-1})	S_{1407}	Spectral index	Notes
201	09 43 52.3	47 4 46	8	12	3		
202	43 56.2	46 24 15	3	42	4		
203	44 6.0	45 3 44	2	286	52		
204	44 20.3	44 50 22	4	180	55		
205	44 26.5	46 0 25	6	27	4		
206	09 44 28.0	46 5 48	e	234	50		Extended 1' towards N
207	44 37.4	49 15 6	4	238	*		5C1.94 ARG 43
208	44 43.6	46 22 3	3	45	4		
209	44 48.8	47 32 20	e	118	20		Extended 2' towards N
210	44 49.5	47 10 28	8	14	3		
211	09 45 8.8	47 46 36	e	675	130		5C1.96 ARG 45 Extended; see map
212	45 8.5	45 58 20	2	88	7		
213	45 11.4	46 12 46	9	17	4		
214	45 14.3	45 46 47	6	39	6		
215	45 17.1	47 43 51	e	67	18		See map
216	09 45 25.6	46 48 40	7	18	3		
217	45 29.0	47 34 52	7	20	4		
218	45 30.4	47 0 54	4	35	4		Slightly extended
219	45 43.7	46 31 49	2	70	5		
220	45 45.5	46 25 3	3	43	5		
221	09 45 57.3	48 6 55	8	27	6		
222	45 57.7	46 48 46	3	46	4		
223	46 6.5	48 26 46	2	175	23		5C1.98 ARG 46
224	46 8.9	46 37 15	e	185	30		
225	46 32.4	45 59 51	8	29	6		

1975MNRAS.171..475P

226	09	46	43.7	45	11	1	2	343	81	
227		46	44.4	47	24	41	4	39	5	
228		46	46.5	46	34	32	8	21	5	
229		46	49.4	47	32	7	7	25	5	
230		47	0.8	46	7	28	e	141	35	Smaller component 2' to W with 0.4 of flux density
231	09	47	4.9	47	26	56	3	51	6	
232		47	17.5	48	49	42	2	322	89	5C1.100 ARG 49
233		47	46.5	48	18	4	4	89	16	
234		48	0.6	45	30	13	7	70	19	
235		48	12.7	49	5	50	8	220	*	5C1.103
236	09	48	17.3	47	26	1	4	61	8	
237		48	50.6	47	34	39	7	39	8	
238		48	53.9	48	19	35	6	90	22	
239		49	12.8	47	20	40	1	219	25	Confused by grating ring
240		49	15.9	46	43	33	4	79	11	
241	09	49	30.3	44	53	60	8	332	*	Confused by grating ring
242		49	37.4	47	15	20	4	87	13	
243		49	42.8	46	52	12	e	81	21	Small extension to NW; confused by grating ring
244		50	23.7	46	39	34	2	223	36	Confused by grating ring
245		50	24.4	47	38	28	5	91	20	Perhaps slightly extended
246	09	50	39.0	45	24	37	6	266	*	
247		51	4.5	46	2	28	4	180	56	Confused by grating ring
248		51	6.8	47	20	13	e	93	35	Confused by grating ring
249		51	30.4	47	50	50	3	313	*	Slightly confused by grating ring
250		51	41.0	47	29	51	4	155	44	

hour angle and causes the beamshape to depart from the ideal elliptical symmetry at the edges of the map; this should not introduce any systematic errors in fitting the position of an ideal beamshape, although it may cause a bias in the fitted flux density.

(ii) Errors in the calibration and geometry of the telescope in observations at higher frequencies (2·7 and 5 GHz) lead typically to uncertainties of about 0″·5 arc in source positions (Smith 1971). At lower frequencies the phase stability is better and the accuracy is limited by errors in the instrumental phase calibration at each aerial separation; in the present survey these were better than 5° and the systematic positional uncertainties less than 1″ arc.

(iii) The formal standard error in the ionospheric refraction correction is about 1″·2 arc, but the actual error may be larger.

The presence of systematic positional errors in the earlier 5C surveys has been suggested by comparison with independent surveys: e.g. van der Kruit & Katgert (1972), comparing 5C 3 with a 1415 MHz survey made at Westerbork, found a mean difference in declination of 3″ arc (Cambridge minus Westerbork); but Parkes & Penston (1973) found no significant discrepancy when comparing 5C 3 positions with those of optical identifications, the difference (optical minus radio) being $\overline{\Delta\alpha} = 0''{\cdot}24 \pm 0''{\cdot}70$, $\overline{\Delta\delta} = -1''{\cdot}22 \pm 1''{\cdot}05$. Differences of this magnitude are consistent with the estimated systematic errors.

3.2 *Flux densities*

The source-finding program produces estimates of the apparent flux densities S' of the sources on the synthesized map; these flux densities have been corrected for the following effects:

(i) The attenuation at the edge of the map due to the envelope response of the individual aerials, which was remeasured after the installation of the new feeds. The details are given in the Appendix.

(ii) The attenuation due to the finite bandwidth of the receivers, which increases towards the edges of the map where the equalization of the signal paths via the two aerials is not correct. The maximum correction is about 20 per cent. A small error recently discovered in the cabling of the telescope has been allowed for in this correction. This error will have affected by a few per cent the measured flux densities of sources near the edges of the earlier 5C regions.

(iii) The attenuation due to the finite time-constant of the receivers, which also is greatest at the edges of the map. This correction does not exceed 2 per cent for any of the sources.

The rms uncertainties in flux density given in Table I (columns 6 and 8) include the contribution of random noise and confusion, which were determined in the Monte Carlo experiments, and an estimate of the uncertainty in the above three correction factors. It should be noted, however, that errors in the measured envelope response are likely to be correlated over large areas. Sources outside the 10 per cent contour of the 408 MHz envelope response, or the 15 per cent contour of the 1407 MHz response, for which the error in flux density may exceed 20 per cent, are marked with an asterisk in Table I.

The flux density scale was established by reference to 3C 48, for which the

following values were assumed:

$$S_{408} = 35 \times 10^{-26} \text{ W m}^{-2} \text{ Hz}^{-1}$$
$$S_{1407} = 15{\cdot}8 \times 10^{-26} \text{ W m}^{-2} \text{ Hz}^{-1}$$

(Kellermann, Pauliny-Toth & Williams 1969; the value for S_{408} being derived by interpolation). The scale adopted here is uniform with the earlier 5C surveys. To be consistent with the absolute scale of Wyllie (Wyllie 1969; Conway & Munro 1972) the 408 MHz flux densities in Table I should be increased by 9 per cent.

The flux densities at the two frequencies have been used to calculate spectral indices $\alpha(408, 1407)$ (column 9), according to the convention $S \propto \nu^{-\alpha}$.

4. COMPARISON WITH OTHER SURVEYS

4.1 *5C 1*

Thirty-one of the sources observed at 408 MHz in 5C 5 are identified with 5C 1 sources by positional agreement, and these are indicated in Table I (column 10). These include all but four of the 5C 1 sources south of 49° declination, and the four excluded would be expected from their 5C 1 flux densities to fall below the 5C 5 limit. None of the sources in common was observed at 1407 MHz in either survey.

There is a small systematic discrepancy between the two sets of positions of these sources. The mean difference (5C 5 − 5C 1) in the right ascensions is $-1^{s}{\cdot}27 \pm 0^{s}{\cdot}13$ (s.e.) and in the declinations $-5''{\cdot}8 \pm 1''{\cdot}6$. There is no systematic variation of this difference with position, in so far as such a variation could be detected in a small sample. Although the difference is rather larger than the estimated errors in either survey, it can perhaps be explained by errors in the ionospheric refraction correction or in the geometry of the telescope assumed for 5C 1.

The 408 MHz flux densities of 15 of the common sources, those that lie within both the 20 per cent contour of the 5C 1 envelope pattern and the 10 per cent contour of the 5C 5 envelope pattern, are compared in Fig. 1. Differences in flux density could arise from the effects of receiver noise, secular variation or polarization (the two surveys were made using orthogonally-polarized receivers); but confusion should affect both surveys equally, except in the case of confusion by grating rings. Fig. 1 shows that, as well as these random differences, there is a systematic difference between the two flux density scales. On average, the 5C 5 flux densities are greater than those of 5C 1, with a mean ratio (weighted according to the estimated variances) of 1·25. The underestimation of the 5C 1 flux densities causes an underestimation in spectral index $\alpha(408, 1400)$ of about 0·2; this accounts for a large part of the difference in mean spectral index found by Maslowski (1972a, 1974) between the 5C 1 and 5C 2 regions (see Section 8). The errors in the 5C 1 flux densities show some positional dependence: considering only the sources within the 10 per cent contour of 5C 5 all the sources with $S(5C\,5)/S(5C\,1) < 1{\cdot}0$ lie to the east of $\alpha = 09^{h}\,40^{m}$, and all but one of those with $S(5C\,5)/S(5C\,1) > 1{\cdot}2$ lie to the west of this line. This is consistent with the results of Condon & Jauncey (1973) and confirms that there were errors in the envelope response correction in the outer parts of the 5C 1 survey. The new observations, however, cannot confirm Condon & Jauncey's suggestion that a similar effect was present in 5C 2. The flux density errors in 5C 1 may be attributed to the difficulty of removing the effects of the primary beam offset and heavy interference with which this early survey was unfortunately afflicted.

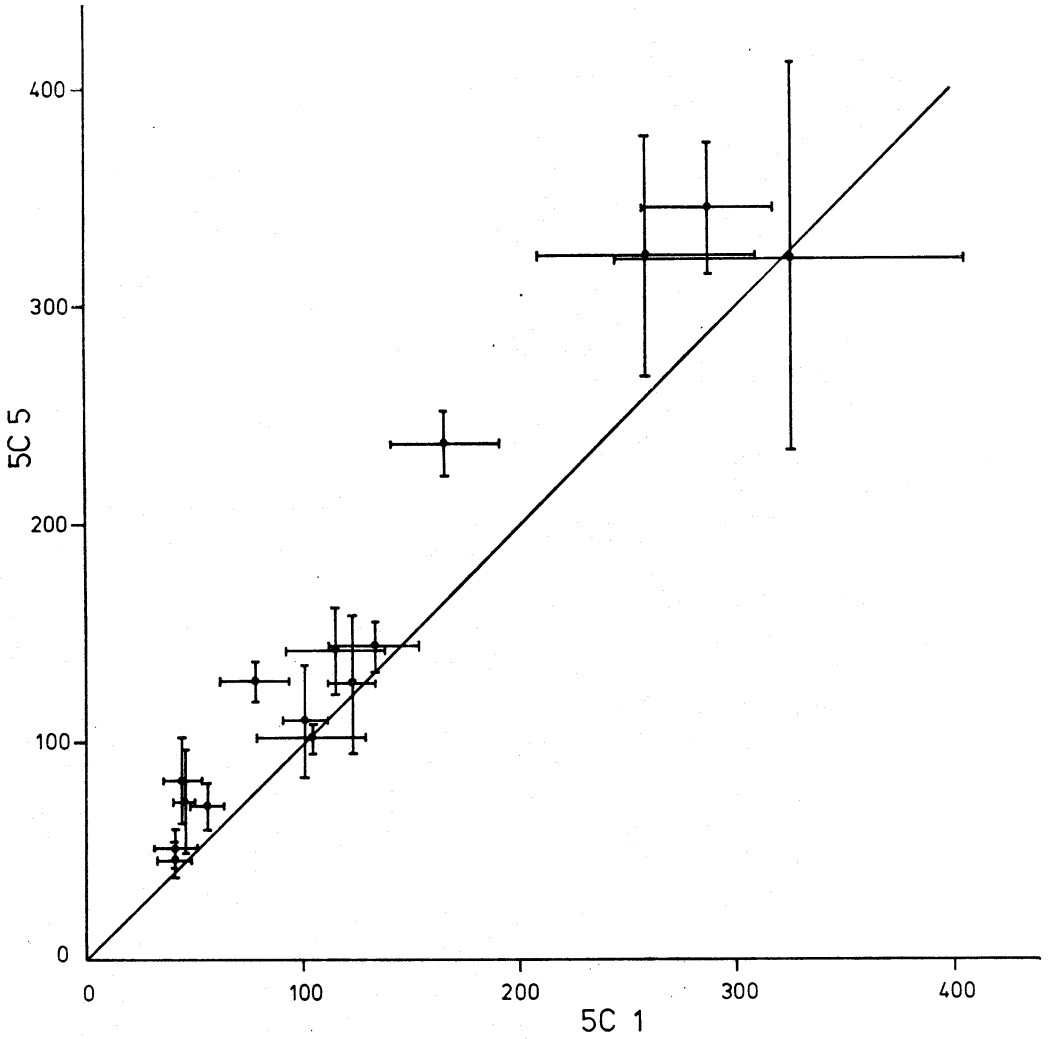

FIG. 1. *Comparison of 408 MHz flux densities measured in the 5C 1 and 5C 5 surveys. The error bars show the quoted errors. The straight line has unit slope. The scales show S_{408} in units of 10^{-29} W m^{-2} Hz^{-1}.*

4.2 *Half-Mile telescope survey at 1421 MHz* (Gillespie, in preparation)

This survey was made with an instrument having the same resolution at 1421 MHz as 5C 1 and 5C 5 at 408 MHz, and was centred midway between the (nominal) centres of 5C 1 and 5C 5. The 5C 5 sources observed are indicated by the symbol ARG in column 10 of Table I. The spectral indices $\alpha(408, 1421)$ computed from the 5C 5 408 MHz flux densities and Gillespie's 1421 MHz flux densities show no dependence on the position of the sources relative to the two map centres. This suggests that there are no gross errors in the envelope correction of either 5C 5 or the Half-Mile survey.

4.3 *The GB survey (1400 MHz)* (Maslowski 1971, 1972a, 1972b)

The resolving power of this survey (HPBW 10′·3 arc in right ascension, 11′·1 arc in declination) is very much worse than that of 5C 5, and the catalogue is limited to sources with $S_{1400} > 90 \times 10^{-29}$ W m^{-2} Hz^{-1}. It is possible to identify some of the GB sources with groups of 5C sources, as Maslowski has done for 5C 1 and 5C 2 sources, but this is an unreliable process, particularly if the results are to be used to derive spectral indices (Condon & Jauncey 1973). It would be more satisfactory

to convolve the 5C 5 map with the beamshape of the GB survey before making the comparison. For the present, no attempt has been made to collate the GB and 5C 5 sources by this method, although Gillespie (1975) has repeated Maslowski's simpler analysis, using the 5C 5 408 MHz flux densities in place of those of 5C 1 in order to compare the spectral properties of the 5C 1/5C 5 and 5C 2 regions (see Section 8).

4.4 *The KPD survey (5 GHz)* (Kellermann *et al.* 1968)

This survey (HPBW $6' \times 6'$) detected some of the brighter 5C 1 sources, including four 5C 5 sources; these are noted in Table I.

5. OPTICAL IDENTIFICATIONS

The positions of the sources in Table I were examined on a copy of the National Geographic Society–Palomar Sky Survey (Plate No. 672) using computer-drawn transparent overlays. In Table II brief descriptions are given of any optical objects which lie within about 2·5 standard deviations of the radio position, the standard deviation being a combination of the error in the radio position (column 4 of Table I) and the positioning error of the overlay, estimated to be about 5″ arc rms. The search area thus defined was about 20″ arc in radius for most sources. The positions of the optical objects are given relative to the radio position, rounded to the nearest 5″ arc, and are omitted when the radio object is extended or the optical object is less than 5″ arc from the radio position. The estimated magnitudes may be in error by $\pm 1^m$.

A total of about 120 objects is listed in Table II, in the fields of 102 of the 250 radio sources. Taking account of the large search areas and the density of ' objects ' on the Sky Survey plates, the fraction of the listed objects that can be attributed to chance coincidences unrelated to the radio sources may be more than two-thirds. To reduce this fraction, we must reduce the search area by improving the accuracy of either the radio positions or the optical positions. A very much smaller number of identifications emerges from identification programmes using more accurate techniques for measuring the optical positions, e.g. Parkes & Penston (1973) examined 209 5C 3 sources and found seven quasar and nine radio galaxy candidate identifications satisfying their positional agreement criterion, with an expected chance coincidence rate of 2·2 quasar candidates and 3·6 galaxies.

Four of the suggested identifications are with bright galaxies listed in the catalogue of Vorontsov-Velyaminov & Krasnogorskaja (1962). All of these are spiral galaxies; three (VV 8-18-19, -22, -33) are identified with unresolved sources apparently coincident with the optical nucleus (respectively 5C 5.58, 82 and 217); the fourth (VV 8-18-13, 5C 5.26) is one of a pair of interacting spiral galaxies, but the radio position does not coincide with the centre of the galaxy and a more likely candidate is a 17^m red object 25″ arc south of the galaxy.

Fifteen of the sources lie in the direction of groups or clusters of galaxies. One of these sources, 5C 5.125, appears to be associated with the cluster 0939·8+4714 listed by Zwicky & Herzog (1966) and described as ' compact, extremely distant '. The radio position is near the edge of the cluster, which has a diameter of about 7′ arc, but it is notable that the radio source has a very steep spectrum ($\alpha(408, 1407) = 1{\cdot}21$). This is an example of the association between steep spectrum and cluster identification that has been noticed by Baldwin & Scott (1973).

TABLE II

Optical objects in the fields of the radio sources

5C 5	
1	20^m blue object 15″ f.
2	19–20^m red object 10″ Np.
4	17^m blue object 15″ N; 18^m red object 15″ p.
11	17^m galaxy in cluster 10″ N.
15	20^m red objects 20″ Sf, 15″ p.
16	18^m blue object 5″ N.
17	19^m blue object 20″ Nf.
22	19^m galaxy in cluster 15″ p.
23	20^m red object 15″ S.
26	17^m red object 5″ Sp, 25″ S of 15^m spiral galaxy VV 8-18-13 (interacting with 8-18-12?)
32	19^m object.
33	20^m red object 15″ Sp.
35	19^m object 5″ N.
38	16^m star 10″ N; 17^m star 60″ Sf within extent of source.
39	19^m red object 5″ N.
42	17–18^m object 15″ Np in a cluster of 20^m objects.
46	19^m red objects 10″ Np, 15″ S.
49	19^m blue object 15″ f.
50	19^m blue object 15″ N, 19^m red object 20″ p.
52	20^m blue object.
53	20^m red object 15″ f.
55	17–18^m blue object 10″ f.
56	18^m object 20″ Sf, 19^m 15″ f, 20^m 5″ p.
57	20^m object 15″ S.
58	Nucleus of 14^m spiral galaxy VV 8-18-19.
59	19^m galaxy?
60	Group of 19–20^m red objects.
63	20^m red object.
67	17^m object 20″ Nf.
70	19–20^m red object 5″ f.
72	Group of 20^m red objects.
74	17^m object 15″ p.
75	19^m red object 5″ N.
79	Two 20^m red objects.
82	14^m edge-on galaxy VV 8-18-22.
84	16^m object 15″ N.
85	Two 18^m galaxies 25″ N.
86	20^m object 10″ p.
90	19^m object 15″ N.
92	18^m red object 25″ Sp.
94	18^m object 15″ S.
99	18^m red object 20″ Sf.
108	Group of 16–17^m galaxies.
109	19^m blue object.
115	20^m red object.
119	18–19^m red object 15″ p.
120	17^m star 15″ S.
121	19^m red object, perhaps in a group.
124	19^m red object in a cluster.
125	Some faint objects, on edge of cluster (see text).
127	19^m red object 15″ p.
129	18–19^m red object.
131	19^m red object 10″ Sp.
132	17^m star.

TABLE II—*continued*

5C 5	
137a	19^m object 15″ Sf.
140	Group of red objects about 20^m.
143	20^m object.
146	20^m object 15″ N.
148	17^m object 5″ p.
151	19^m blue object 15″ N.
152	18–19^m red object 10″ Sp.
153	19^m blue object.
154	17^m galaxy 10″ Sf; 18^m galaxy 10″ Np.
156	18^m galaxy 15″ S (one of a pair).
157	19^m blue object.
160	18–19^m red object 5″ f.
163	17^m red object.
165	19^m red object 10″ Sp.
167	19^m red object 20″ Sp.
170	18^m object 15″ p.
171	17–18^m galaxy 10″ Nf.
172	18^m star 10″ f.
174	Group of 19–20^m red objects.
177	17–18^m blue object.
178	17^m object 15″ Sp.
179	20^m red object 15″ Nf.
180	16^m star.
181	Four objects 10″ f: two 17–18^m stars? and two 19^m galaxies.
185	19^m object.
187	19^m galaxy 10″ Sp, in a cluster.
188	A number of faint red objects within the extent of the source.
194	20^m red object.
196	20^m red object.
199	20^m red object 15″ p.
202	18^m star.
203	20^m red object.
208	19^m object 15″ f.
209	18^m red object 15″ S.
211	19^m object.
215	18^m blue object 10″ p.
217	Nucleus of 15^m galaxy VV 8-18-33.
218	19^m red galaxy + similar galaxy 10″ p.
223	Two 18^m galaxies 5″ f in a cluster.
227	18–19^m red object in a small group 5″ S.
228	13–14^m galaxy, centre 15″ f.
230	18^m object 5″ S.
235	16^m star.
237	20^m red object 15″ f.
241	Several faint red objects in the search area.
242	17^m star 15″ f.
244	20^m object 5″ f.
249	20^m object 15″ Sf.

6. NOTES ON SOME OF THE SOURCES

Contour maps of the sources which were appreciably resolved at either frequency are shown in Fig. 2. In some cases, the maps show that sources which were listed separately in Table I should be regarded as components of a single source, joined by low-brightness emission.

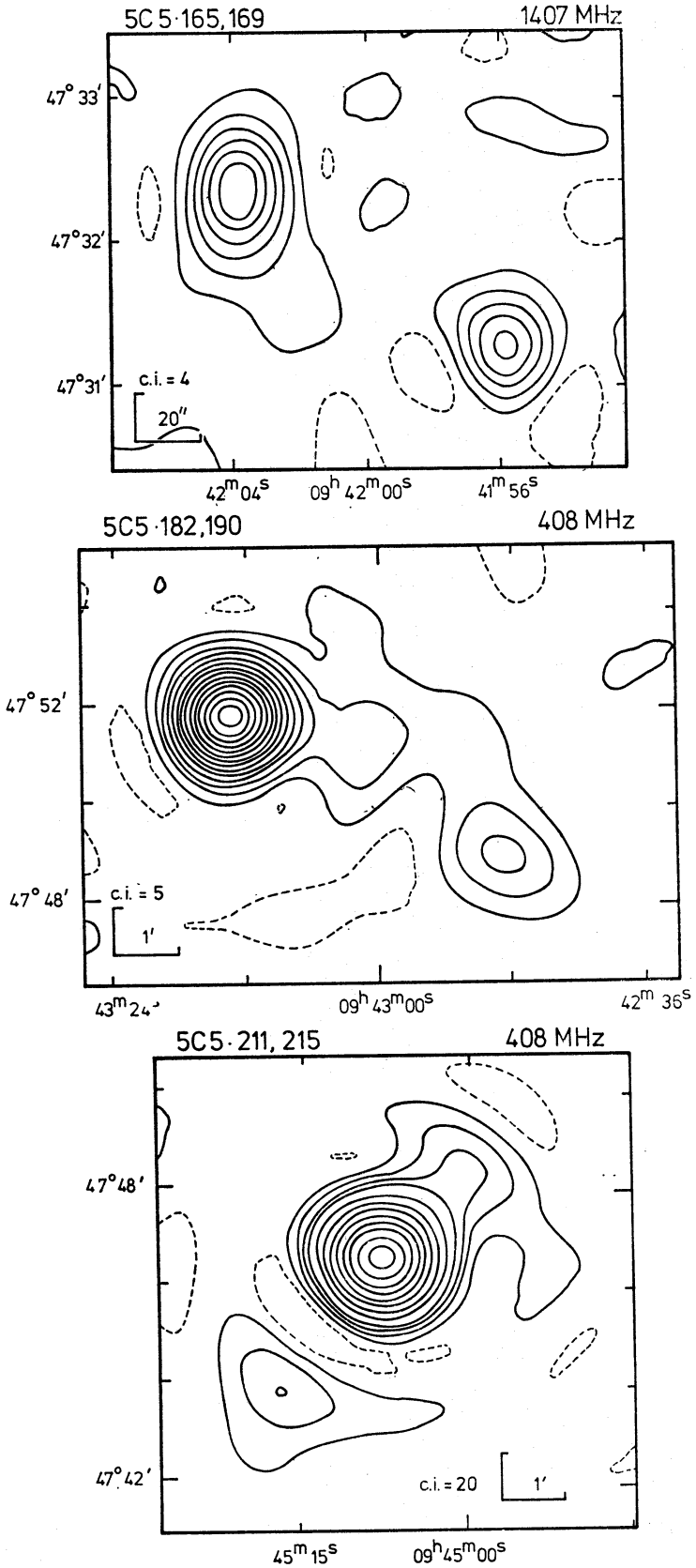

FIG. 2. *Contour maps of some of the sources. The declination scales have been compressed by a factor sin 47° so that the beamshape appears circular. The scales are indicated by L-shapes. The contour interval (c.i.) is shown for each map in units of* 10^{-29} *W* m^{-2} *Hz*$^{-1}$ *per beam area; the first full contour is at approximately one-half the contour interval above zero, and the dotted contours are negative. For 5C 5.211, 215 alternate contours above the fourth are omitted.*

5C 5.165 and 169

Both sources are resolved at 1407 MHz, and their proximity suggests that they are the two components of a double source. There are several optical objects in the field, including a 19^m red object and a 17^m star.

5C 5.182 and 190

The weaker component (182) is appreciably resolved. The flux density of the 'central' component is included with that of the unresolved stronger component (190) in Table I. The angular separation of the two peaks of emission is about 5′ arc; because of the large size, it is difficult to make a convincing optical identification.

5C 5.211 and 215

211 has an extension to the NW and with 215 appears to form a triple source with a strong central component. The contour map is distorted by the sidelobes of the central component. There is a 19^m red stellar object coincident with the central component.

5C 5.131

This source is of interest for its spectrum. Its flux density at 1407 MHz is 65×10^{-29} W m^{-2} Hz^{-1}, but it was not detected at 408 MHz, leading to an upper limit on its spectral index $\alpha(408, 1407) \leqslant -1{\cdot}74$ (Table IV). It was observed at 5000 MHz with the Cambridge 5-km telescope: its flux density at this frequency is $(78 \pm 4) \times 10^{-29}$ W m^{-2} Hz^{-1}, and it is unresolved (HPBW 2″ arc). The steep inverted low-frequency spectrum therefore flattens at higher frequencies, with $\alpha(1407, 5000) = -0{\cdot}05$. The source is tentatively identified with a 19^m red object (Table II).

7. SOURCE COUNTS

The flux density distribution (source count) of the 5C 5 sources at each of the two frequencies was computed by the method outlined by Katgert *et al.* (1973). That is, the contribution of each source was weighted by the inverse of the area over which it could have been observed, determined from the noise level, the chosen completeness limit (in this case six times the rms noise level), and the flux density correction factors discussed in Section 3. The weighting functions for the two frequencies are shown in Fig. 3. Two corrections to the derived source counts were made, both of which may be regarded as modifications of the weighting function:

(i) *The population-law-dependent correction for confusion and noise.* This correction was evaluated by the method of Murdoch *et al.* (1973), approximating the flux density error distribution by a Gaussian curve, and using the correction factors given by Murdoch *et al.* (Table 2 of their paper) for a power-law cumulative source count $N(S) \propto S^{-1}$, which is a fair approximation in the range of interest. The weight attached to each source was reduced by the correction factor appropriate to the signal-to-noise ratio with which it was observed. The corrections derived in this way are slightly larger than those obtained with the series-expansion method of Bennett (1962).

(ii) *Obscuration of weak sources by stronger.* If a weak source falls within about 1′ arc of a stronger source it will not have been detected separately; this means that the area over which a source could have been observed is slightly smaller than

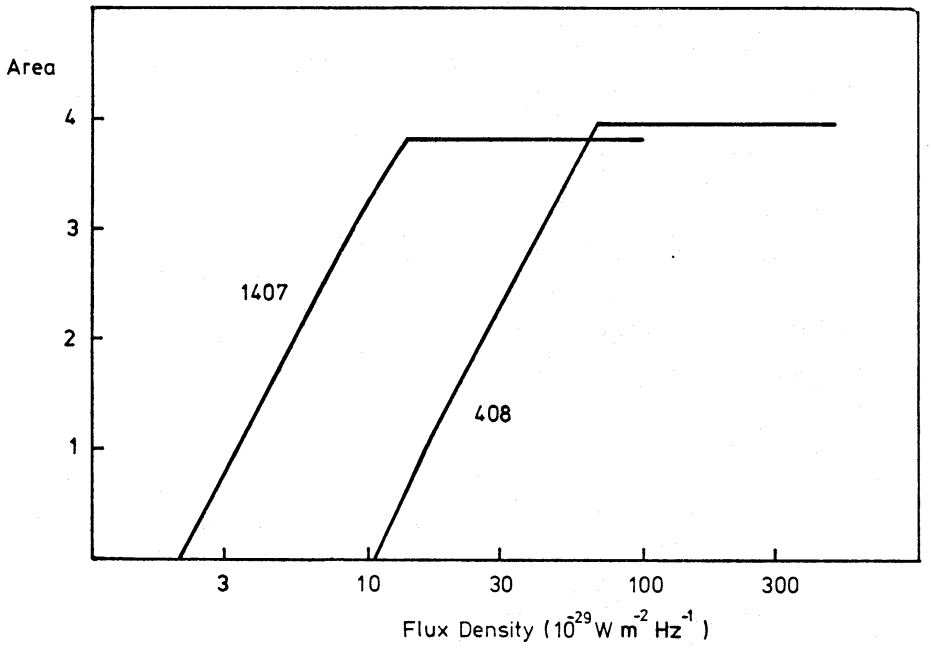

FIG. 3. *The area of sky observed as a function of flux density limit (six times the rms noise level) at the two frequencies. The units of area are* 10^{-4} *sr* (1407 *MHz*) *or* 10^{-3} *sr* (408 *MHz*).

the value derived earlier. The necessary correction was calculated from a preliminary determination of the source count. The concomitant overestimation of the flux density of the obscuring source is simply a case of confusion, and is accounted for by correction (i). The possibility that two sources separated by more than 1′ arc may be the unrecognized components of a single source was ignored; that is, the associations noted in Section 6 were here regarded as separate sources.

There is a third error which affects the source count at low flux densities: the omission of weak extended sources. An extended source may have a total flux density greater than the completeness limit, while its peak flux density is too small for inclusion in the source-list. It is very difficult to correct this error, owing to the difficulty of determining the number of such sources. If the number were known, the correction could be included by adapting the Monte Carlo method used to derive the correction (i). The error is reduced by evaluating the source counts to a higher flux density limit than the nominal limit of the source-list; it is for this reason that sources with a signal-to-noise ratio of less than 6 have been omitted from the source-count analysis. For some resolved sources, however, the total flux density is up to three times the flux density found by the beamshape-fitting programme, which suggests that the source-counts will be unreliable below about 15 times the noise level (that is, $2{\cdot}6\times10^{-28}$ W m^{-2} Hz^{-1} at 408 MHz or $5{\cdot}4\times10^{-29}$ W m^{-2} Hz^{-1} at 1407 MHz) particularly at 1407 MHz where an appreciable fraction of sources is resolved. In view of the probable error, the source-counts at the lowest flux densities should be treated with caution.

The source counts from the 5C 5 survey are presented in Table III in numerical form and in Fig. 4 in the form of ' normalized ' differential source counts $\Delta N/\Delta N_0$; the corrected number ΔN of sources in each flux density interval has been divided by the number ΔN_0 to be expected if the cumulative source count were of the form $N(S) \propto S^{-1.5}$.

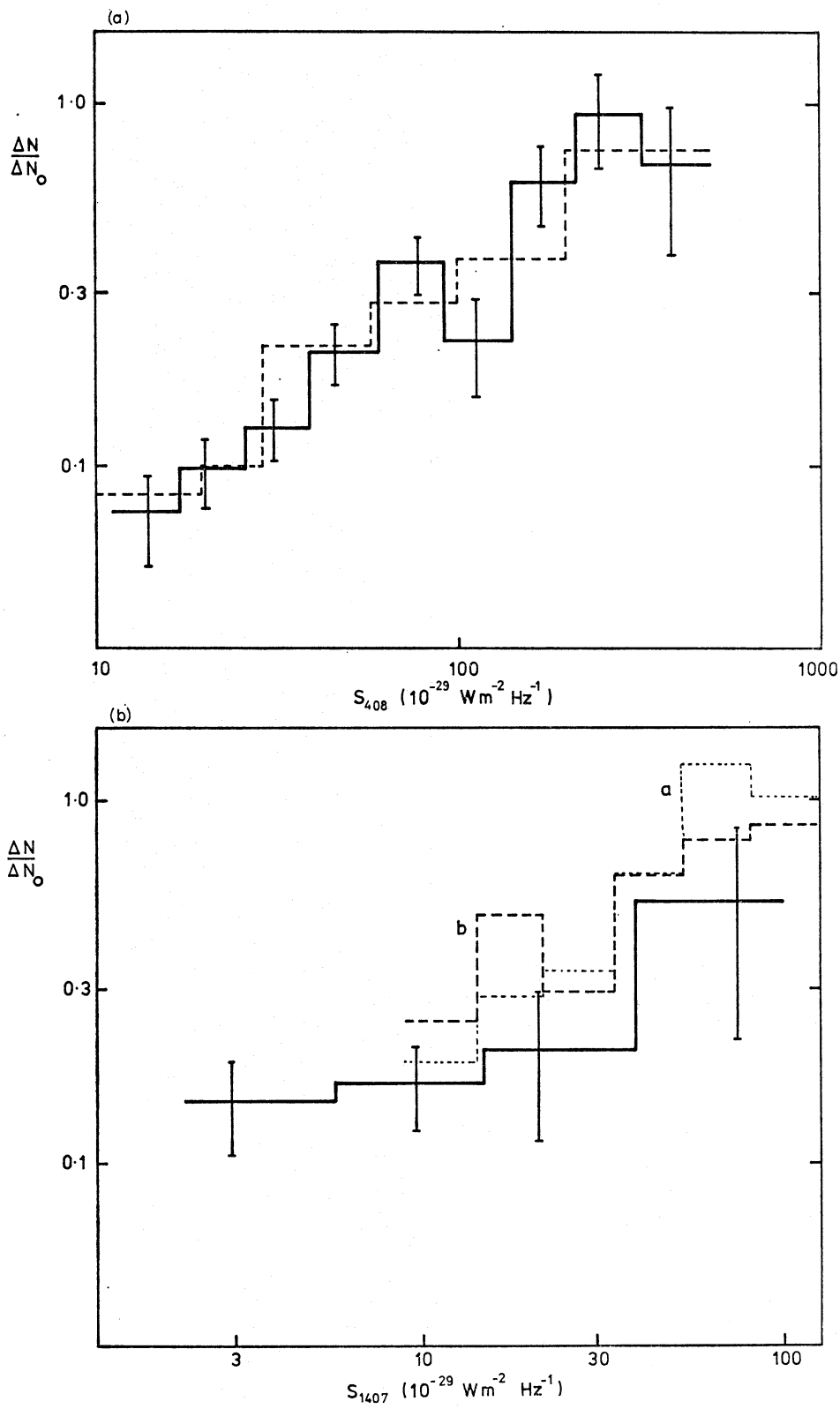

FIG. 4. *The source counts from the 5C 5 survey.* (*a*) *One hundred and sixty-eight sources observed at 408 MHz with* $11 \leqslant S_{408} < 500 \times 10^{-29}$ *W m*$^{-2}$ *Hz*$^{-1}$. *Sources with a signal-to-noise ratio less than 6, or outside the 15 per cent contour of the reception pattern, have been omitted. The arbitrary normalizing count is* $N_0 = 750\, sr^{-1} (S/10^{-26}\, W\, m^{-2}\, Hz^{-1})^{-1\cdot5}$. *The error bars represent* $m^{1/2}$ *statistical errors, based on the number m of sources contributing (see Table III*(*a*)). *The dotted line is the 5C 2 count, with error bars omitted for clarity (Longair 1974).* (*b*) *Thirty-four sources observed at 1407 MHz, with* $2\cdot2 \leqslant S_{1407} < 100 \times 10^{-29}$ *W m*$^{-2}$ *Hz*$^{-1}$; *sources outside the 20 per cent contour of the reception pattern have been omitted. The normalizing count is* $N_0 = 150\, sr^{-1}\ (S/10^{-26}\, W\, m^{-2}\, Hz^{-1})^{-1\cdot5}$. *The dotted lines are* (*a*) *the 1421 MHz count of Gillespie (1975) and* (*b*) *the 1415 MHz count of Katgert* et al. (1973).

TABLE III

Source counts

	S	m	$\Delta N'$	ΔN	$\Delta N/\Delta N_0$
(a) 408 MHz	11·0				
		13	0·218	0·225	0·0735
	16·8				
		22	0·155	0·158	0·0973
	25·7				
		25	0·108	0·109	0·127
	39·3				
		29	0·093	0·094	0·206
	60·0				
		34	0·087	0·087	0·360
	91·7				
		11	0·028	0·028	0·220
	140·1				
		16	0·041	0·041	0·608
	214·1				
		13	0·033	0·033	0·935
	327·2				
		5	0·013	0·013	0·681
	500·0				
(b) 1407 MHz	2·2				
		12	1·766	1·643	0·149
	5·7				
		14	0·450	0·440	0·167
	14·8				
		5	0·131	0·130	0·206
	38·5				
		3	0·079	0·079	0·522
	100·0				

Explanation: S is flux density (10^{-29} W m^{-2} Hz^{-1}); m is the number of sources observed in the flux density range; $\Delta N'$ is the equivalent number in 10^{-5} sr; ΔN is the corrected equivalent number; ΔN_0 is the expected number if $N(S) \propto S^{-1.5}$ (see caption to Fig. 4).

(a) *408 MHz*

The source count is plotted in Fig. 4(a) with the results derived from the 5C 2 survey (Pooley & Ryle 1968; Longair 1974). It is clear that the two histograms coincide, within the statistical uncertainty: there is no significant difference in the flux-density distribution of sources between 5C 2 and 5C 5 (in the range $11 \leqslant S_{408} < 500 \times 10^{-29}$ W m^{-2} Hz^{-1}). In view of this agreement the distributions from the two areas can be combined to give a distribution which, to the best of our knowledge, is typical of the whole sky; this is shown in Fig. 5, with the data of Mills, Davies & Robertson (1973) at higher flux densities—for uniformity the 5C flux densities have been increased by 9 per cent to conform to the scale used by Mills *et al.* (that of Wyllie 1969). There is good agreement in the region of overlap ($220 \leqslant S_{408} < 500 \times 10^{-29}$ W m^{-2} Hz^{-1}) between the small areas 5C 2 and 5C 5 (total about 0·008 sr) and the larger area from which the results of Mills *et al.* are derived (0·160 sr at declination about $-20°$). There is no evidence from the present results that, at 408 MHz, sources are not uniformly distributed over the sky, at least in the region of convergence of the source counts below the maximum of dN/dN_0.

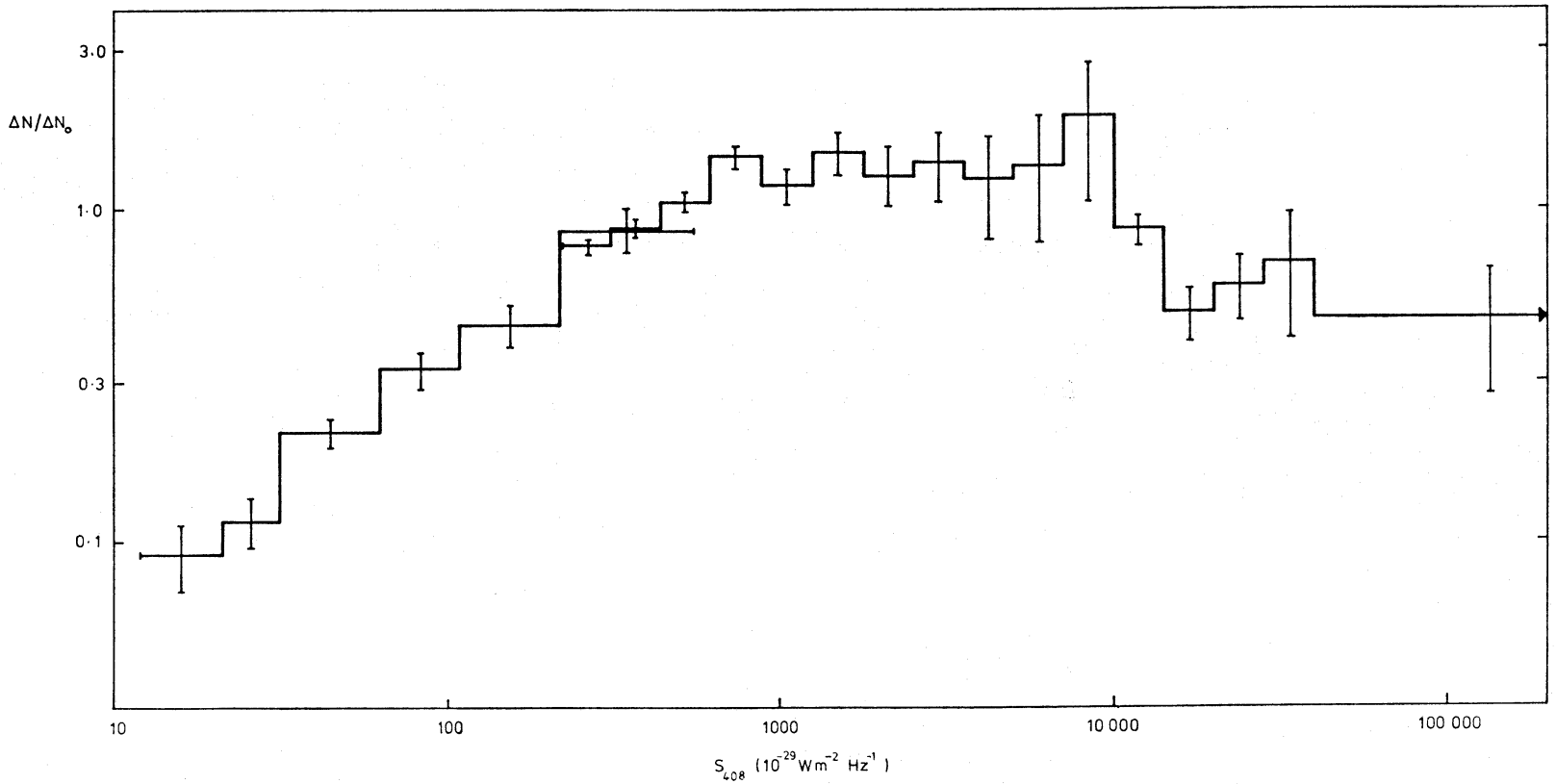

FIG. 5. *Combined differential source counts from 5C 5, 5C 2 and Mills* et al. (1973; *i.e. the Molongo MC1 survey for* $220 \leqslant S_{408} < 10\,000 \times 10^{-29}$ *W m*$^{-2}$ *Hz*$^{-1}$, *and a whole-sky compilation for* $S_{408} \geqslant 10^{25}$ *W m*$^{-2}$ *Hz*$^{-1}$). *The normalization is to* $N_0 = 750$ *sr*$^{-1}$ $(S/10^{-26}$ *W m*$^{-2}$ *Hz*$^{-1})^{-1\cdot5}$ *but note that in this Figure the flux densities are on the scale of Wyllie so that both flux densities and normalization differ from those of Fig.* 4(*a*). *The lowest flux density range* $(12\cdot0 \leqslant S_{408} < 21\cdot3 \times 10^{-29}$ *W m*$^{-2}$ *Hz*$^{-1}$) *includes only the 5C 5 sources.*

(b) *1407 MHz*

The number of sources observed at this frequency is small but, allowing for the large statistical errors, the source count shown in Fig. 4(b) agrees fairly well with those of Katgert *et al.* (1973) and Gillespie (1975) shown in the same Figure. The anisotropy in source counts at 1400 MHz found by Machalski, Zieba & Maslowski (1974) in the GB survey suggests that the 5C 5 1407 MHz source count might not be typical of the whole sky. Gillespie (1975), however, found no significant difference between the 1420 MHz source counts from his survey area, adjacent to the area surveyed at 1407 MHz in 5C 5, and those from other 5C regions. There is an apparent change in the slope of the source count in Fig. 4(b) at low flux densities, but in view of the possible errors mentioned earlier, this cannot be regarded as significant.

8. SPECTRA

The spectral indices $\alpha(408, 1407)$ of the sources which were observed at both frequencies are given in column 9 of Table I. Formal errors can be derived from the uncertainties in the flux density measurements (columns 6 and 8) by assuming that the errors in measurement at the two frequencies are uncorrelated, which is valid for receiver noise and for confusion by sidelobes and grating rings (which change their position with frequency of observation). Typical uncertainties in spectral index are about 0·1.

In order to obtain a complete sample of spectral indices for sources selected at 1407 MHz, S_{408} was estimated for the 18 sources which fall below the completeness limit at 408 MHz. These estimates, or in some cases upper limits corresponding to four times the rms noise level, are given in Table IV, with the corresponding spectral indices.

TABLE IV

Sources observed at 1407 MHz but not at 408 MHz

5C 5	Estimated S_{408}* (10^{-29} W m^{-2} Hz^{-1})	$\alpha(408, 1407)$
89	7·7	0·10
98	<7·6	<0·72
101	<7·6	<0·56
111	<7·7	<0·57
112	<7·7	< −0·44
118	<7·5	<0·92
124	<7·5	<0·99
129	<7·6	<0·78
131	<7·5	< −1·74
132	<7·4	<0·94
138	8·3	0·85
143	<7·5	<0·18
144	8·5	0·90
147	9·4	0·67
149	7·6	0·70
150	8·1	0·68
162	<7·8	<0·44
174	<8·0	<0·48

* The upper limits are four times the rms noise level.

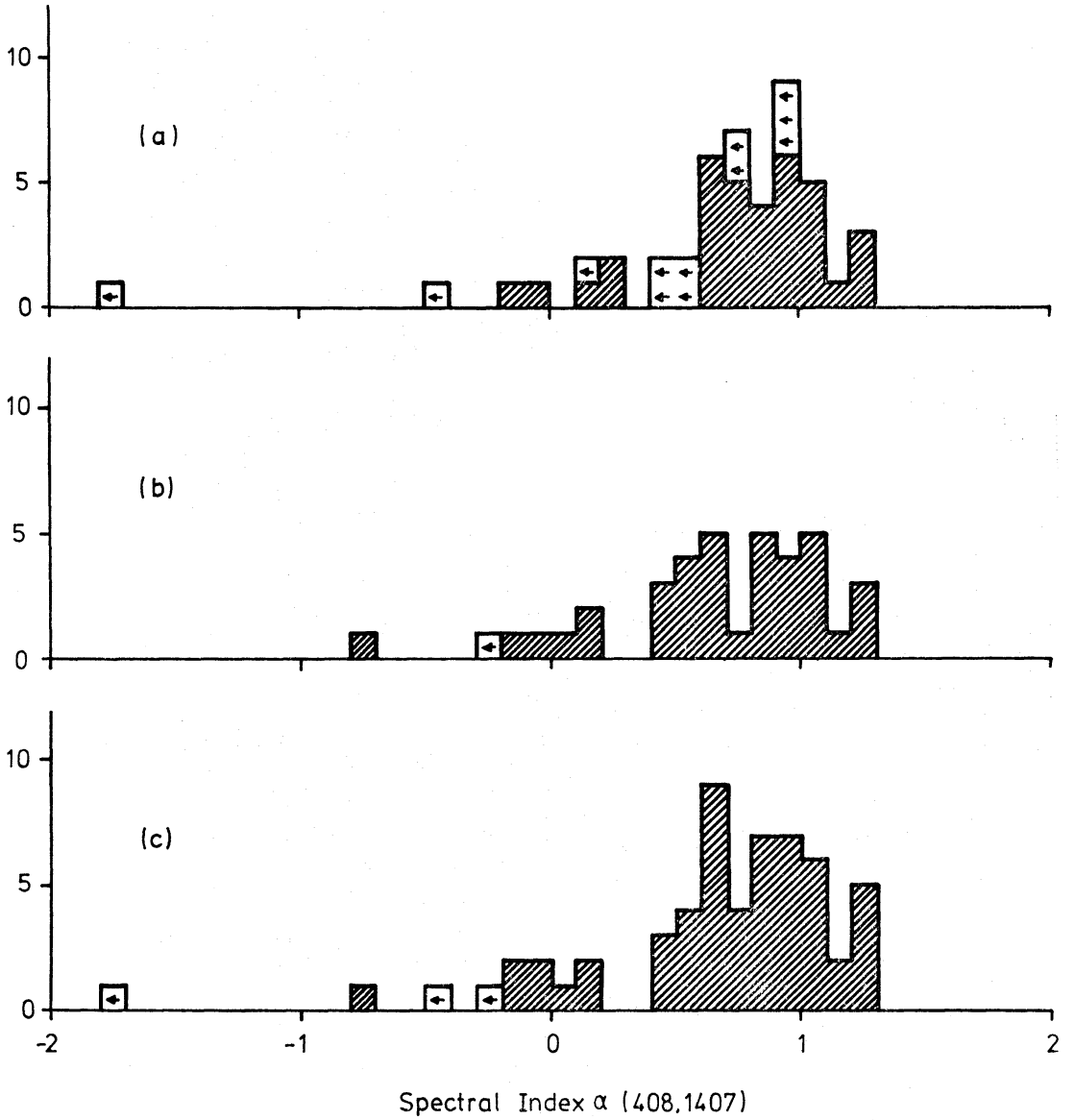

FIG. 6. *Spectral distributions of sources observed in the 5C 5 surveys; arrows indicate upper limits to spectral index.* (*a*) *All sources observed at* 1407 *MHz in 5C 5.* (*b*) *Sources with* $10 \leqslant S_{1407} < 200 \times 10^{-29}$ *W m*$^{-2}$ *Hz*$^{-1}$ *observed in 5C 2, 3 and 4* (*Willson* 1972). (*c*) *The distribution* (*b*) *together with the 20 sources from* (*a*) *having* $10 \leqslant S_{1407} < 200 \times 10^{-29}$ *W m*$^{-2}$ *Hz*$^{-1}$.

The spectral index distribution for the complete sample of 47 sources is shown in Fig. 6(a). This sample excludes the sources 5C 5.191 and 193, which lie outside the 15 per cent contour of the 1407 MHz reception pattern, and assumes 5C 5.165 to be part of 5C 5.169 as mentioned in Section 6. Note that the sample is not complete above a fixed limiting flux density, because of the variation of the limiting flux density across the field, and is therefore not an example of a 'spectral index distribution ${}^{S}f_{\nu}(\alpha)$' according to the definition of Fanaroff & Longair (1973). The distribution can be 'corrected' by weighting the sources according to the area observed, but it is then dominated by a small number of weak sources which have large weights, and is difficult to assess statistically. Note that the sensitivity at 408 MHz is almost uniform over the region surveyed at 1407 MHz, so that the

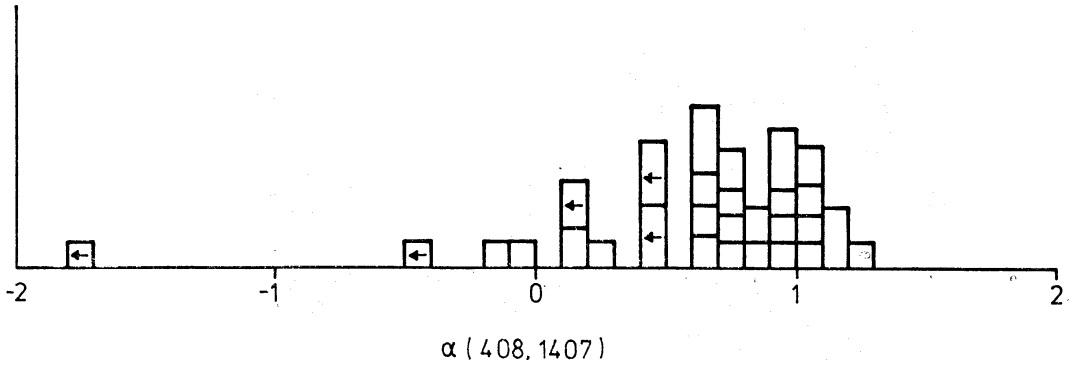

FIG. 7. *Weighted spectral index distribution for the 29 sources observed at 1407 MHz with flux density greater than* 4×10^{-29} *W m*$^{-2}$ *Hz*$^{-1}$ *and signal-to-noise ratio greater than six.*

uncorrected distribution is unbiased, and only differs significantly from the corrected distribution if there is a strong dependence of ${}^{S}f_{1407}(\alpha)$ on flux density S over the range represented ($2 \leqslant S_{1407} < 250 \times 10^{-29}$ W m^{-2} Hz^{-1}). A corrected distribution is shown in Fig. 7, where sources fainter than 4×10^{-29} W m^{-2} Hz^{-1} have had to be omitted to prevent the weight of any source exceeding three times the minimum weight, and sources with a signal-to-noise ratio less than six (at 1407 MHz) have also been omitted.

The distribution of Fig. 6(a) is very similar to that derived by Willson (1972) from the three surveys 5C 2, 5C 3 and 5C 4 for sources with $10 \leqslant S_{1407} < 200 \times 10^{-29}$ W m^{-2} Hz^{-1} which is shown in Fig. 6(b)*; the 20 5C 5 sources in this flux density range were added to Willson's distribution to derive Fig. 6(c). Some characteristic statistics of the three distributions (Fig. 6(a)–(c)) are tabulated in Table V.

There is no evidence for anisotropy from the 5C spectral index distributions. Indeed, the 5C 5 survey shows the same 'excess' of steep-spectrum sources at low flux densities that Willson found in 5C 2, 3 and 4. The difficulties of explaining this excess have been discussed by Willson (1972) and by Fanaroff & Longair (1972). It cannot be explained simply by selection against flat-spectrum sources. Fanaroff & Longair noticed a correlation between steep spectrum and large angular size in Willson's sample; this correlation, however, is not obvious in 5C 5. Six of the 47 sources in Fig. 6(a) are extended (see Table I), but all have $0{\cdot}7 < \alpha < 1{\cdot}1$, and they do not include the sources with the steepest spectra.

The good agreement of the spectral index distribution of the present sample with that of Willson is to be contrasted with the assertion of Maslowski (1972a, 1974) that, for $S_{1400} > 150 \times 10^{-29}$ W m^{-2} Hz^{-1}, the distributions of α(408, 1400) and of α(1400, 2695) are markedly different in the 5C 1 and 5C 2 survey areas, with generally flatter spectra occurring in 5C 1. For α(408, 1400) the effect is largely due to the errors in the 5C 1 survey, but these do not affect the α(1400, 2695) distributions, and there still appears to be real anisotropy. However, the present observations show that the 'spectral anomaly' associated with the 5C 1 area either does not extend to the adjacent region surveyed at 1407 MHz in 5C 5, or is confined to sources with $S_{1407} > 150 \times 10^{-29}$ W m^{-2} Hz^{-1}, of which there are

* Willson's spectral indices were calculated according to the flux density scale (KPW) used in the present survey.

TABLE V

Statistics of the spectral index distribution

Sample	No. of sources	Mean	Median	Fraction $\alpha<0{\cdot}5$	Mean and standard deviation (excluding $\alpha<0{\cdot}3$)	
1. All sources observed at 1407 MHz in 5C 5	47	$0{\cdot}67\pm0{\cdot}07$	0·79	$0{\cdot}21\pm0{\cdot}06$	$0{\cdot}85\pm0{\cdot}03$	0·20
2. $10<S_{1407}<200\times10^{-29}$ W m^{-2} Hz^{-1} (5C 2, 3, 4) (Willson 1972)	38	$0{\cdot}72\pm0{\cdot}06$	0·77	$0{\cdot}26\pm0{\cdot}07$	$0{\cdot}83\pm0{\cdot}04$	0·25
3. $10<S_{1407}<200\times10^{-29}$ W m^{-2} Hz^{-1} (5C 2, 3, 4, 5)	58	$0{\cdot}63\pm0{\cdot}07$	0·75	$0{\cdot}24\pm0{\cdot}06$	$0{\cdot}85\pm0{\cdot}03$	0·23

The mean is unduly affected by the sources of negative spectral index and the median and mean (excluding $\alpha\geqslant0{\cdot}3$) are more characteristic statistics. The latter has been chosen because there is a clear division in all three samples between $\alpha<0{\cdot}3$ and $\alpha\geqslant0{\cdot}4$. The statistics have been calculated by including upper limits and true estimates with equal weight.

few in the present sample. The spectra of the 5C 1 sources which were re-observed at 408 MHz in 5C 5 are discussed by Gillespie (1975) who used the 5C 5 flux densities and new measurements at 1421 MHz (see Section 4.2) to re-derive the distribution of $\alpha(408, 1400)$ for part of the 5C 1 region (his Fig. 2). He found no significant differences in spectral distribution between the 5C 2, 5C 3, 5C 4 and 5C 5 areas. Gillespie also repeated Maslowski's analysis, using the new 408 MHz flux densities from 5C 5 in place of the less satisfactory results of 5C 1; although there is still a difference in mean spectral index ($\bar{\alpha}(5C\,5) = 0{\cdot}57 \pm 0{\cdot}06$, $\bar{\alpha}(5C\,2) = 0{\cdot}79 \pm 0{\cdot}06$), this difference is not incompatible with the expected sampling fluctuations. The reduction of the difference in $\bar{\alpha}$ is due primarily to the difference in flux density scale between 5C 5 and 5C 1 (Section 4.1); but it should be noted that there may be a further scaling difference of a few per cent between 5C 5 and 5C 2.

9. CONCLUSIONS

The following are the principal results of the 5C 5 survey:

(a) Two hundred and thirty sources have been observed at 408 MHz; of these about 150 have not been observed before.

(b) Fifty-two sources have been observed at 1407 MHz, including 32 of those observed at 408 MHz.

(c) Suspected errors in the flux densities observed in the 5C 1 survey have been confirmed by direct observation.

(d) There is no evidence for anisotropy in the radio source distribution. The flux density distributions of 5C 5 and 5C 2 are in good agreement, and the spectral index distribution of 5C 5 is similar to those of the earlier 5C surveys.

ACKNOWLEDGMENTS

I thank the many members of the Mullard Radio Astronomy Observatory who have been involved in the running of the One-Mile telescope and in the analysis of the observations described here, in particular Dr G. G. Pooley. I am grateful to the referee for helpful comments. Mr A. R. Gillespie kindly allowed me to use his results before publication. I am indebted to the Science Research Council for a Research Studentship.

REFERENCES

Baldwin, J. E. & Scott, P. F., 1973. *Mon. Not. R. astr. Soc.*, **165**, 259.
Bennett, A. S., 1962. *Mon. Not. R. astr. Soc.*, **125**, 75.
Condon, J. J. & Jauncey, D. L., 1973. *Astrophys. J.*, **184**, L33.
Conway, R. G. & Munro, R. E. B., 1972. *Mon. Not. R. astr. Soc.*, **159**, 21P.
Fanaroff, B. L. & Longair, M. S., 1972. *Mon. Not. R. astr. Soc.*, **159**, 119.
Fanaroff, B. L. & Longair, M. S., 1973. *Mon. Not. R. astr. Soc.*, **161**, 393.
Gillespie, A. R., 1975. *Mon. Not. R. astr. Soc.*, **170**, 541.
Katgert, P., Katgert-Merkelijn, J. K., Le Poole, R. S. & van der Laan, H., 1973. *Astr. Astrophys.*, **23**, 171.
Kellermann, K. I., Pauliny-Toth, I. I. K. & Davies, M. M., 1968. *Astrophys. Lett.*, **2**, 105.
Kellermann, K. I., Pauliny-Toth, I. I. K. & Williams, P. J. S., 1969. *Astrophys. J.*, **157**, 1.
Kenderdine, S., Ryle, M. & Pooley, G. G., 1966. *Mon. Not. R. astr. Soc.*, **134**, 189.
Longair, M. S., 1974. *IAU Symposium No.* 63, p. 93, ed. M. S. Longair, Reidel Publishing Co., Dordrecht.
Machalski, J., Zieba, S. & Maslowski, J., 1974. *Astr. Astrophys.*, **33**, 357.
Maslowski, J., 1971. *Astr. Astrophys.*, **14**, 215.

Maslowski, J., 1972a. *Astr. Astrophys.*, **16,** 197.
Maslowski, J., 1972b. *Acta Astr.*, **22,** 227.
Maslowski, J., 1974. *Astr. Astrophys.*, **36,** 395.
Mills, B. Y., Davies, I. M. & Robertson, J. G., 1973. *Austr. J., Phys.*, **26,** 417.
Murdoch, H. S., Crawford, D. F. & Jauncey, D. L., 1973. *Astrophys. J.*, **183,** 1.
Neville, A. C., Windram, M. D. & Kenderdine, S., 1969. *Observatory*, **89,** 186.
Parkes, A. G. & Penston, M. V., 1973. *Mon. Not. R. astr. Soc.*, **162,** 117.
Pooley, G. G., 1969. *Mon. Not. R. astr. Soc.*, **144,** 101.
Pooley, G. G. & Kenderdine, S., 1968. *Mon. Not. R. astr. Soc.*, **139,** 529.
Pooley, G. G. & Ryle, M., 1968. *Mon. Not. R. astr. Soc.*, **139,** 515.
Smith, J. W., 1971. *Nature Phys. Sci.*, **232,** 150.
van der Kruit, P. C. & Katgert, P., 1972. *Astrophys. Lett.*, **11,** 181.
Vorontsov-Velyaminov, B. A. & Krasnogorskaja, A., 1962. *Morphological catalogue of galaxies*—I, Moscow University Press.
Willson, M. A. G., 1970. *Mon. Not. R. astr. Soc.*, **151,** 1.
Willson, M. A. G., 1972. *Mon. Not. R. astr. Soc.*, **155,** 385.
Wyllie, D. V., 1969. *Mon. Not. R. astr. Soc.*, **142,** 229.
Zwicky, F. & Herzog, E., 1966. *Catalogue of galaxies and of clusters of galaxies*—III, California Institute of Technology.

APPENDIX

THE ENVELOPE RESPONSE OF THE ONE-MILE TELESCOPE

The polar diagrams of the three primary aerials of the telescope were measured by making observations of an intense point source, one aerial of each interferometer pair being offset by a variable angle from the direction of the source. The combined envelope responses of the three aerials for the two frequencies, taking into account the grading used in the synthesis, are given in Fig. A1, which shows radial profiles in the East–West direction. In the North–South direction the 1407 MHz profile is identical, and the 408 MHz profile has the same shape but is 10 per cent wider; limited observations in other directions of offset are consistent with the response having elliptical symmetry. The rms error in the measured values of the response is estimated to be 3 per cent. The direction of maximum response is slightly offset from that assumed—in the present survey the maximum is 2′·6 East and 0′·4 North of the quoted survey centre.

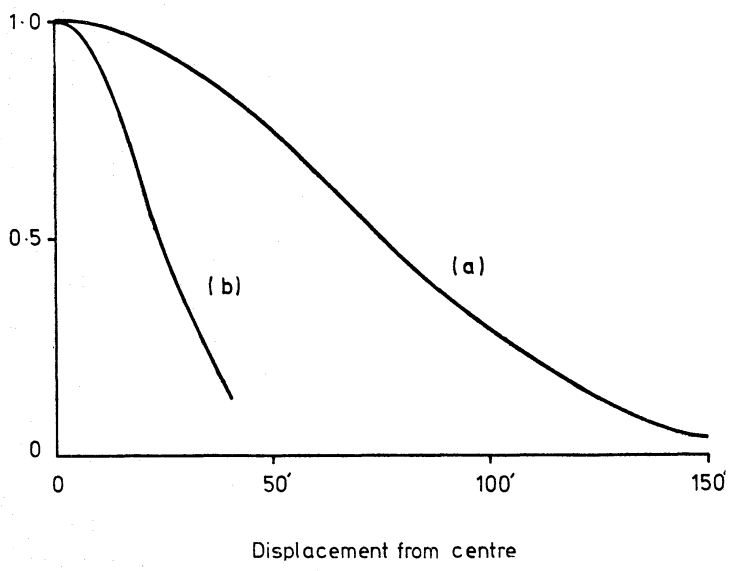

FIG. A1. *East–West radial profiles of the envelope responses of the One-Mile telescope at 408 MHz (a) and 1407 MHz (b).*